

THE EFFECTS OF CORONAL REGIONS ON THE X-RAY FLUX AND IONIZATION CONDITIONS IN THE WINDS OF OB SUPERGIANTS AND OF STARS

JOSEPH P. CASSINELLI

Washburn Observatory, University of Wisconsin-Madison

AND

GORDON L. OLSON

Free University of Brussels, Belgium

Received 1978 July 12; accepted 1978 September 19

ABSTRACT

The anomalously strong O VI and N V lines in O stars and the C IV lines in B supergiants may be due to Auger ionization by X-rays from a thin coronal zone at the base of the cool stellar winds. We determine the size of a corona that is necessary to produce the overall ionization conditions in ζ Pup as has been deduced by Olson from line profile analyses. In the ionization balance calculations we account for the diffuse radiation field in the wind and for the large optical depths in the He II continuum due to radiative and Auger ionization edges of abundant elements. The X-ray flux transmitted through the wind is calculated and compared with upper limits derived for ζ Pup observations from *ANS* and *Uhuru* satellites. It is found that a coronal zone with a temperature of 5×10^6 K and a volume emission measure of 10^{58} cm^{-3} can produce the required ionization in a wind having a temperature of 30,000–35,000 K. The emergent X-ray flux bears little resemblance to the coronal emissivity because of the opacity of the wind. The X-ray flux nearly reaches the upper limits derived from the *ANS* observations and, at several energy bands, should be detectable by the *HEAO B* satellite. A simplified analysis of the Auger ionization process is developed and applied to other Of and OB supergiants. We find that the model can explain the presence of C IV and Si IV in supergiants with effective temperatures as low as 12,000 K and can explain the appearance of O VI and N V lines in early type supergiants as late as B0.5 and B2, respectively.

Subject headings: stars: coronae — stars: early-type — stars: supergiants — stars: winds

I. INTRODUCTION

Copernicus satellite spectra show strong lines with P Cygni profiles from resonance lines of O VI and N V in all O stars and Si IV in B supergiants (Snow and Morton 1976). *Skylab* observations (Parsons *et al.* 1978) have shown that C IV appears strongly in supergiants with effective temperature as low as 15,000 K. These high stages of ionization were not expected to persist over such wide ranges of spectral types if the winds are in radiative equilibrium.

A possible explanation of the high stages of ionization in O and B stars has been offered by Lamers and Morton (1976), Lamers and Snow (1977), and Lamers and Rogerson (1978). They suggest that the wide range of ionization can be explained if the electron temperature in the stellar winds is of order 10^5 K. Lamers and Morton (1976) analyzed the P Cygni profiles of ζ Pup and deduced that the O⁺⁵ and N⁺⁴ ions exist over a spatially extended region (many stellar radii) and concluded that the chromospheric temperatures also exist throughout this region. To contrast these with the models that have hot coronal zones ($T > 10^6$), we refer to the extended 10^5 K models as "warm wind models."

The existence of temperatures near 10^5 K in the

winds has been questioned, however. Cassinelli, Olson, and Stalio (1978) argued in favor of cool winds on the basis of their theoretical fits to the H α profiles in ζ Ori (O9.7 Ia) and ζ Pup. In particular, they found that a mass loss rate exceeding the single scattering limit, $\dot{M}_{\text{max}} = L/v_{\infty}c$, would be required if the temperature is 2×10^5 K. On the other hand, models having wind temperatures appropriate for radiative equilibrium, $0.6-0.9T_{\text{eff}}$, lead to fits of the H α profile with mass loss rates below the limit.

If the wind is at the "cool" radiative equilibrium temperatures of 3 to 4×10^4 K for ζ Pup, a different explanation must be found for the production of the observed O⁺⁵ ions. Photoionization by radiation shortward of 100 Å is a possible cause, but only if it is significantly larger than that expected to arise from the photosphere at these wavelengths. A hot coronal zone could provide the necessary flux of hard radiation.

Coronal zones at the base of the winds of early type stars were suggested by Hearn (1975). He analyzed the emission and absorption equivalent widths of the H α profile in ζ Ori and deduced that there is a coronal region extending to 2 stellar radii, caused presumably by the deposition of mechanical flux as in the solar corona. In contrast to the solar case, there should be a

rapid drop in temperature above the energy deposition region because the densities are so large ($\sim 10^{10} \text{ cm}^{-3}$) that radiative recombination is effective in cooling the gas.

However, Hearn did not address the problem of explaining the anomalous ionization by using hard radiation from the coronal zone. Natta *et al.* (1975) noted a serious problem with such an explanation. They found that the wind of ζ Pup should be optically thick at the O^{+4} to O^{+5} ionization edge at 109 \AA and concluded that, if hard radiation is responsible for the ionization, it must be produced locally, and not arise from a coronal zone at the base of the wind. They suggested that there are hot filaments with temperatures of order 10^6 K distributed throughout the wind, produced perhaps by flow instabilities.

In spite of this potential difficulty, a study of the observational consequences of the coronal models of the type suggested by Hearn has been the goal of this and two previous papers. Cassinelli and Hartmann (1977) showed that coronal zones give rise to a broad bump in the infrared near $30 \mu\text{m}$, above the excess expected from the wind itself. Cassinelli, Olson, and Stalio (1978) have reanalyzed Hearn's study of the $\text{H}\alpha$ profile in ζ Ori, using the Sobolev line transfer method. They concluded that the coronal zone must be very thin and that the velocity at the top of the corona must be small compared to the photospheric escape velocity. It is the purpose of this paper to determine if hard radiation from the coronal zone at the base of the stellar wind could produce the anomalously high stages of ionization in a cool stellar wind, and at the same time satisfy observational constraints on the X-ray fluxes. The analysis will first be applied to ζ Pup (O4f) because of the large amount of observational and semiempirical data available. The ultraviolet resonance lines have recently been fitted by Olson (1978) with theoretical profiles to provide the degree and spatial distribution of ionization of C, N, O, Si, and S. Severe upper limits on the X-ray flux from ζ Pup have been determined from the *ANS* satellite (Mewe *et al.* 1975) and from the *Uhuru* satellite (Giacconi *et al.* 1974).

In § II is described the basic working model of a coronal zone surrounded by a cool, i.e., radiative equilibrium, wind. The constraints imposed by the analysis of the ultraviolet profiles in ζ Pup by Olson (1978) are presented, and limits to acceptable emergent X-ray fluxes are derived.

In § III, a simplified theory for deriving the ionization structure of an optically thick wind is developed. The wind is found to be very thick in the extreme-ultraviolet so that the dominant stages of ionization are produced by the diffuse radiation field in the cool stellar wind. In the soft X-ray region the main source of opacity is the K-shell ionization of oxygen which varies with frequency as $\nu^{-2.6}$ and is nearly independent of whatever is the dominant stage of ionization. As a result it is rather easy to analyze the transfer of X-rays through the wind. The X-rays produce trace amounts of high stages of ionization of C, N, and O by the Auger mechanism in which two electrons are

ejected following K-shell absorption. A more detailed analysis is then developed for treating the ionization structure in an optically thick stellar wind that accounts for the transfer of the diffuse radiation field as well as the attenuation of the coronal X-rays. These techniques are then applied to a study of ζ Pup.

In § IV the theory is extended to discuss the B supergiants which also show anomalously high stages of ionization in their spectra. In these cooler stars the dominant stages of ionization in the cool winds shift from triply to singly ionized stages. Since the Auger mechanism produces anomalously large abundances of ions two stages above the dominant stage, we predict the range in effective temperature for which certain ultraviolet lines should be anomalously strong. These predictions are compared with *Copernicus* and *Skylab* observations and are found to be in excellent agreement. As the O VI observations were the original impetus for proposing various wind models, a more detailed discussion of the production of O^{+5} in stars near the critical effective temperature (below which no O^{+5} would be expected in a corona cool wind model) is presented.

A summary is given in § V.

II. THE ASSUMED MODEL AND THE OBSERVATIONAL CONSTRAINTS ON THE CORONAL EMISSION FOR ζ PUPPIS

a) *The Hybrid, Corona-plus-Cool-Wind Model*

The model we wish to test is one having a thin coronal region at the base of the outflow, surrounded by a stellar wind which has a relatively cool temperature of 3 to $4 \times 10^4 \text{ K}$ as is appropriate for a gas in radiative equilibrium. The observed ultraviolet lines are formed in the cool wind region, but the degree of ionization in this wind may be somewhat enhanced by the hard radiation from the coronal zone.

We assume that the wind has a velocity distribution of the form

$$v^2(r) = v_0^2 + v_1^2(1 - R_*/r), \quad (1)$$

where R_* is the stellar radius and v_0 and v_1 are chosen so that the flow has a terminal velocity of 2660 km s^{-1} and $v_0 = v_1/20$. To determine the density distribution, we assume a mass loss rate, \dot{M} , to be $8 \times 10^{-6} \mathcal{M}_\odot \text{ yr}^{-1}$ and use the conservation of mass equation

$$\dot{M} = 4\pi\rho(r)v(r)r^2 \quad (2)$$

to derive the run of density in the wind.

A mass loss rate of about $8 \times 10^{-6} \mathcal{M}_\odot \text{ yr}^{-1}$ was derived for ζ Pup from an analysis of the $\text{H}\alpha$ profile by Cassinelli, Olson, and Stalio (1978) and by Conti and Frost (1977). Recently ζ Pup has been detected at radio wavelengths by Morton and Wright (1978) and a mass loss rate of about $6.2 \times 10^{-6} \mathcal{M}_\odot \text{ yr}^{-1}$ was derived from the observed flux assuming the wind to be at a temperature of $2 \times 10^5 \text{ K}$. With a Gaunt factor appropriate for $T \approx 35,000 \text{ K}$, the derived mass loss rate is $7.1 \times 10^{-6} \mathcal{M}_\odot \text{ yr}^{-1}$. A velocity law

of the form of equation (1) was found by Olson (1978) to produce reasonably good fits to the ultraviolet resonance line profiles. There are other velocity laws, say with a lower rate of increase, that also satisfy this requirement. The uncertainties in $v(r)$ do not produce large errors in the abundances determined from the profile, nor in the basic conclusions of this paper.

For the stellar flux distribution, we assume a sequence of Planck functions. Holm and Cassinelli (1977) have shown that the visual and ultraviolet flux distributions, as measured by *OAO 2*, and the angular diameter data for ζ Pup by Davis *et al.* (1970), can be explained with a star having an effective temperature of 42,000 K and a mass loss rate of about $8 \times 10^{-6} M_{\odot} \text{ yr}^{-1}$. Therefore we will assume that the emergent flux distribution is that of a 42,000 K Planck function over most of the emergent spectrum. We allow for the expected drop in the emergent flux at the He II $n = 1$ absorption edge by adopting a distribution of a 35,000 K Planck function at, and near, the edge at 228 Å. Because of the dependence of low stages of ionization, such as C^{+2} and Si^{+3} , on the photospheric field and not on coronal emission, we found it possible to achieve the observed ionization abundances only by reducing the photospheric brightness temperatures from 42,000 K to 35,000 K in the region 228–280 Å. The photospheric field is likely to be deficient in this spectral region because of the confluence of the He II Lyman lines, and because of the larger number of resonance lines of heavier elements in that wavelength range. A similar modification of the far-ultraviolet flux of hot stars was needed by Kirkpatrick (1972) and Bohlin, Harrington, and Stecher (1978) to explain the ionization conditions in planetary nebulae. It can be justified because of the large uncertainties that exist in theoretical predictions from model atmospheres of hot stars, as has been recently discussed by Hummer (1977).

For our purposes the coronal zone is completely specified by the coronal temperature T_c and emission measure integrated over the volume of the coronal region

$$EM_c = \int_{R_*}^{R_c} N_e^2 d \text{Vol.} \quad (3)$$

We assume that the coronal region has a temperature of $T_c = 5 \times 10^6$ K and use the emissivity of a coronal gas as has been calculated by Kato (1976). The data for a 5×10^6 K gas is presented in graphical and tabular form in that paper. A major contribution to the coronal radiation field is in emission lines. We have chosen to integrate the emission over bands of about 5–10 Å so as to produce a smoothed coronal emissivity that is more convenient for the radiative ionization integrations. The emergent spectrum from the star plus corona is displayed in Figure 1. The knee in the coronal emission at high frequencies occurs near $h\nu/kT_c = 1$. Thus, if the assumed coronal temperature were increased, the knee would be shifted linearly to larger frequencies. We have chosen to use $T_c = 5 \times 10^6$ K because it is a rather typical coronal

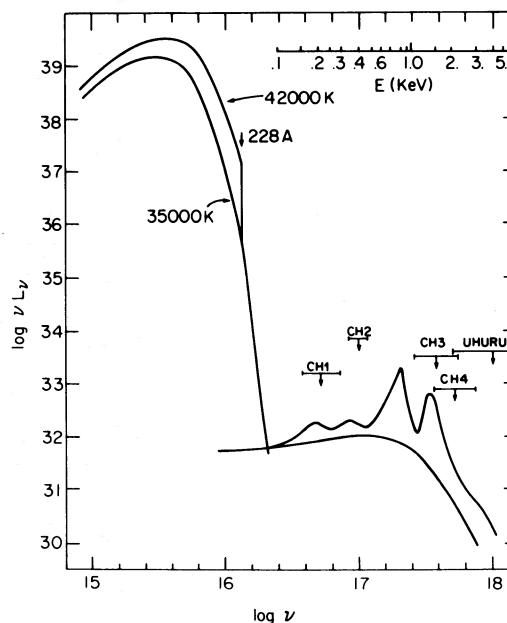


FIG. 1.—The assumed form of the radiation field emergent from the photosphere and coronal zone for ζ Pup. The photospheric field is that of a 42,000 K blackbody longward of 228 Å and of a 35,000 K blackbody just shortward of 228 Å. The coronal emission shown at higher energies is from Kato (1976). The underlying coronal continuum is free-free emission, and the excess emission is due to spectral lines. The coronal distribution shown here is for the case with coronal temperature $T = 5 \times 10^6$ K and a coronal emission measure $EM_c = 10^{56} \text{ cm}^{-3}$. The upper limits of the X-ray flux from ζ Pup as derived from the *ANS* satellite's Channel 1 to Channel 4 detector are indicated, as is the *Uhuru* survey upper limit.

temperature and it produces sufficient flux beyond the K-shell ionization edges, near 10^{17} Hz, for the production of O^{+5} .

The coronal emission measure, EM_c , is the fundamental parameter that we shall adjust to produce the required degree of ionization. For the flux distribution shown in Figure 1, the emission measure is 10^{56} cm^{-3} . If the wind were optically thin, this value of EM_c would be sufficient to produce the required O^{+5} abundance.

b) Constraints on the Permissible X-Ray Flux

An attempt to detect ζ Pup at X-ray wavelengths was made by the *ANS* satellite, and the upper limits for the count rate were derived by Mewe *et al.* (1975) for several bands in the energy region 0.16 to 3 keV. In addition, the region of the sky containing ζ Pup was scanned in the *Uhuru* X-ray survey and was not found to have detectable X-ray emission. This puts an upper limit of 10 counts s^{-1} in the 1–6 keV range.

The energy response functions of the *ANS* detectors (Mewe 1976) can be used to derive detector sensitivities \mathcal{S} (ergs $\text{cm}^{-2} \text{ count}^{-1}$), for various input flux distributions. In Table 1 are given the count-rate upper limits, r , in counts per second for channels 1 to 4 of *ANS* and the sensitivities to a flat spectrum as well as results for X-ray luminosities and interstellar optical depths.

TABLE 1
X-RAY OBSERVATIONS OF ζ PUPPIS

Satellite	ΔE (keV)	\bar{E} (keV)	Sensitivity (ergs cm ⁻² count ⁻¹)	r (counts s ⁻¹)	νL_ν (ergs s ⁻¹)	τ_ν (ISM)
<i>ANS:</i>						
Ch 1.....	0.16-0.284	0.25	2.6×10^{-11}	< 0.27	< 1.2×10^{33}	1.23
Ch 2.....	0.32-0.456	0.41	8.7×10^{-11}	< 0.08	< 6.6×10^{33}	0.26
Ch 3.....	1.05-2.25	1.6	1.1×10^{-9}	< 0.09	< 3.3×10^{33}	0.02
Ch 4.....	1.45-3.00	2.2	3.3×10^{-10}	< 0.07	< 7.9×10^{32}	0.00
<i>Uhuru</i>	2.00-6.00	4.0	1.7×10^{-11}	< 10.0	< 4.1×10^{33}	0.00

The flux observed by the *ANS* satellite is

$$\mathcal{F} = \mathcal{S}r \text{ (ergs cm}^{-2} \text{ s}^{-1}\text{)}. \quad (4)$$

After correcting for the extinction of the interstellar medium to X-rays, τ_x , one can derive upper limits to the X-ray luminosity in the various detector pass bands, as

$$L_x = 4\pi d^2 \mathcal{S}r \exp(+\tau_x). \quad (5)$$

Here d is the distance to ζ Pup (~ 450 pc, Lamers and Morton 1976).

The interstellar optical depth to X-rays in the various *ANS* bands can be calculated using the cross sections of Cruddace *et al.* (1974) and the measured column densities to ζ Pup. Using *Copernicus* spectra, Bohlin (1975) derived a column density for atomic hydrogen of 9.7×10^{19} cm⁻². Morton and Dinerstein (1975) derived a molecular hydrogen column density of 2.8×10^{14} cm⁻². From an analysis of high-resolution measurements of the interstellar H α recombination line, Reynolds (1976) derived a column density of ionized hydrogen of $\lesssim 2.7 \times 10^{20}$ cm⁻². Assuming helium to be neutral where hydrogen is atomic and assuming He to be singly ionized where the H α recombination line is formed, we derived the interstellar optical depths given in Table 1. The estimate for the channel 1 optical depth agrees well with that of Lamers and Morton (1976). The resulting X-ray upper limits are plotted in Figure 1.

c) The Degree of Ionization in ζ Puppis

The degree and spatial distribution of the ionization in the stellar wind can be derived from theoretical fits to unblended ultraviolet resonance lines. Olson (1978) has calculated theoretical profiles for resonance lines using the Sobolev escape probability method. He derives families of profiles that are characterized by the total optical depth of the line, the assumed velocity distribution, and an index describing the spatial distribution of the ion forming the line. The spatial distribution of the ion is parametrized by the index β , such that the ratio of the number density of the ion, N_i , to the electron number density, N_e , is given by

$$\frac{N_i(r)}{N_e(r)} = \left(\frac{N_i}{N_e}\right)_B \left(\frac{r}{r_B}\right)^\beta, \quad (6)$$

where r_B is the radius at a reference point near the

base of the flow. A summary of Olson's results for the fractional degree of ionization ($g_i = N_i/N_{e,i}$) at $2R_*$ and for the spatial index β are given in Table 2 for several ions of interest. For ions having large column densities, the profile is "saturated," i.e., unaffected by further increase in column densities, and for such ions it is possible to set only upper limits on the ionization fraction.

In an optically thin wind there should be an increase in the degree of ionization in the outward direction. This is because of the dependence of ionization on electron density in the radiative ionization equilibrium equation:

$$N_{i+1}N_e\alpha = N_i \int \frac{4\pi}{h\nu} a_\nu J_\nu d\nu \quad (7)$$

$$\approx N_i W \int \frac{4\pi}{h\nu} a_\nu \exp(-\theta_\nu) F_\nu d\nu, \quad (8)$$

where α is the recombination coefficient, a_ν is the absorption cross section, θ_ν is the optical depth of the wind measured from the base of the flow outward, F_ν is the stellar flux, and W is the dilution coefficient. Since $W \propto 1/r^2$ and $N_e \propto (vr^2)^{-1}$, one gets $N_{i+1}/N_i \propto v$ in an optically thin wind. As the velocity increases outward, there should be a monotonic increase of the higher stages of ionization and a decrease of the lower stages with radial distance from the star. A similar argument holds for the Auger ionizations which produce O⁺⁵ from O⁺³.

In optically thick winds, the flux from the star decreases as $\exp(-\theta_\nu)$. Hence the integral on the right-hand side of equation (8) might decrease more

TABLE 2
IONIZATION STRUCTURE AT $2R_*$ IN ζ PUPPIS DERIVED FROM FITTING LINE PROFILES

Ion	β	$g_i(2R_*)$
C ⁺²	-3.	2.6×10^{-3}
C ⁺³	-1. *	$> 5.3 \times 10^{-3}$
N ⁺²	-2.	1.2×10^{-2}
N ⁺³	+0.3	0.25
N ⁺⁴	+1. *	$> 3.1 \times 10^{-3}$
O ⁺⁵	0. *	7.9×10^{-4}
Si ⁺³	-1.	8.6×10^{-4}
S ⁺³	-1.	2.3×10^{-2}
S ⁺⁵	-2.	1.3×10^{-2}

* Values for β could not be determined from the profile, but were chosen, as shown, for theoretical reasons.

rapidly than N_e and cause the higher stages of ionization to decrease with increasing radius.

We have calculated the degree of ionization in the stellar wind accounting for the radiative and collisional ionization, Auger ionization, and radiative and dielectronic recombination. As did Lamers and Morton (1976) and Natta *et al.* (1975), we make the nebular approximation that all ions are in the ground level. For the ζ Pup models we calculated the degree of ionization and opacities of He, C, N, O, Ne, Mg, Si, and S using the solar abundances of Withbroe (1971).

We used the radiative ionization cross sections collected by Osterbrock (1974) and augmented these for higher stages of ionization from the references given in Aldrovandi and Péquignot (1973) and the more recent cross sections of John and Morgan (1974). For K-shell ionizations we used the cross sections of Daltabuit and Cox (1972). The method of Weisheit (1974) was used to modify the statistical equilibrium calculations so as to include the Auger ionization process, and for simplicity we assumed that two electrons are ejected following every K-shell ionization. This assumption is correct for ions with less than 10 electrons such as those of C, N, and O, but is only approximate for Si and S. The collisional ionization rates of Seaton (1964) were used, and the radiative and dielectronic recombination rates were calculated using the formulae of Aldrovandi and Péquignot (1973).

The basic logic of the program for the solution of the matrix of rate equations and the collisional and recombination data were kindly provided to us by Lamers (1975a).

III. IONIZATION CONDITIONS IN THE OPTICALLY THICK WIND OF ζ PUPPIS

a) *A Simplified Theory for Auger Ionization in an Optically Thick Wind*

In the corona plus cool wind model the O^{+5} is produced primarily through the Auger process whereby two electrons are ejected from the dominant stage of ionization, O^{+3} , following the absorption of an X-ray photon. The process also works for other ions and may be able to explain the anomalous ionization seen in O stars and in B supergiants. In this section we develop a simple equation for the fractional abundance of anomalously high stages of ionization that can be produced. The theory requires that the dominant stage of ionization be two stages below the observed anomalous stage, because only a small fraction of these "parent" ions are expected to be ionized in the Auger process. The determination of the dominant stage is somewhat difficult because of the dependence on the diffuse radiation field, but the results are not especially controversial and in this section we will assume that the dominant stages of ionization are known. We focus our attention, instead, on the dependence of the Auger process on the optical depth in the wind and on the coronal emission measure and coronal temperature.

There is a broad frequency region in which the wind is very thick because of bound-free opacity of abundant ions. If the winds of Of stars and OB supergiants are cool, they are optically thick at frequencies extending from the He⁺ edge at 1.3×10^{16} Hz to frequencies somewhat beyond the K-shell ionization edge of oxygen at 1.4×10^{17} Hz. The effects of the radiation field in this frequency range will be discussed below. Here we are only interested in radiation at frequencies beyond the K-shell edges that produce Auger ionization. This simplifies the analysis a great deal because at these high frequencies the only important sources of opacity are K-shell ionizations of carbon, nitrogen, and oxygen, and these opacities are nearly independent of the number of electrons in the outer shells (Daltabuit and Cox 1972). Thus we need not be concerned with the ionization structure of the wind, and the opacity depends only on the total abundances of C, N, and O.

The attenuation optical depth measured outward from the corona at R_c to radius r is

$$\theta_v(r) = \sum_{\text{CNO}} \kappa_v \int_{R_c}^r \rho dr, \quad (9)$$

where κ_v is the opacity per gram, which can be derived from the cross section in Daltabuit and Cox (1972). These have the general form $a_v = a_0(\nu_0/\nu)^s$, where ν_0 is the threshold frequency for K-shell ionization. In particular for C, N, and O we have

$$\begin{aligned} a_v(\text{C}) &= 1.0 \times 10^{-18} (7.2 \times 10^{16}/\nu)^{2.50} \text{ cm}^2, \\ a_v(\text{N}) &= 0.71 \times 10^{-18} (1.0 \times 10^{17}/\nu)^{2.54} \text{ cm}^2, \\ a_v(\text{O}) &= 0.50 \times 10^{-18} (1.4 \times 10^{17}/\nu)^{2.60} \text{ cm}^2. \end{aligned} \quad (10)$$

Using the atomic abundances given by Withbroe (1971) and expressing frequencies in units of the oxygen K-shell edge, $x = \nu/(1.4 \times 10^{17})$, the opacities per gram at frequencies beyond 1.4×10^{17} Hz are

$$\begin{aligned} \kappa_x(\text{C}) &= 29.2 x^{-2.50}, \\ \kappa_x(\text{N}) &= 14.3 x^{-2.54}, \\ \kappa_x(\text{O}) &= 140. x^{-2.60}. \end{aligned} \quad (11)$$

The mass column density from R_c to r may be expressed in terms of velocity at r , by noting that equation (1) leads to the transformation

$$v \frac{dv}{dr} = v_1^2 \frac{R_c}{2r^2}, \quad (12)$$

and thus with equation (2)

$$\int_{R_c}^r \rho dr = \frac{2\dot{M}}{4\pi R_c} \frac{[v(r) - v_0]}{v_1^2}, \quad (13)$$

where \dot{M} is the mass loss rate from the star, and R_c is the radius at the base of the cool wind where the velocity equals v_0 . For the ζ Pup model parameters given earlier, the optical depth of the entire wind at the K edge of oxygen, i.e., at $x = 1$, is $\theta_1(\infty) = 26.0$ and

the optical depth decreases with frequency roughly as $x^{-2.6}$ reaching unity at $\nu = 5 \times 10^{17}$ Hz or 2 keV.

To focus attention on the dependence of the ionization structure on the coronal temperature, we note that the flux distribution of the corona, as seen in Figure 1, can be represented by a simple multiple of the underlying bremsstrahlung continuum,

$$\beta_c F_0 \exp(-h\nu/kT_c),$$

where β_c is a factor to account for line emission from the corona, and F_0 is chosen to fit the bremsstrahlung continuum. An adequate fit to the coronal flux distribution of Figure 1 is

$$F_\nu = EM_c \cdot \beta_c \times 3.5 \times 10^{-67} \exp(-h\nu/kT_c). \quad (14)$$

For the flux distribution shown in Figure 1, the line correction factor is $\beta_c \approx 13$, over the frequency region beyond 1.4×10^{17} .

At the frequencies producing K-shell ionization the only significant contribution to the mean intensity is the diluted and attenuated coronal radiation:

$$J_\nu = WF_\nu \exp(-\theta_\nu). \quad (15)$$

The ionization equilibrium equation which describes the formation of the trace ion El^{P+2} from the parent ion El^P , by the Auger process is

$$N(El^{P+2})N_e\alpha(T_e) = N(El^P) \int_{\nu_{El}}^{\infty} \frac{4\pi}{h\nu} a_\nu J_\nu d\nu, \quad (16)$$

where $\alpha(T_e)$ is the recombination rate from El^{P+2} to El^{P+1} , $N_e(r)$ is the local electron density, and ν_{El} is the threshold frequency for K-shell ionization. Again letting g be the fractional ionic abundance, equation (16) can be rewritten as

$$\frac{g(El^{P+2})}{g(El^P)} \alpha(T_e) = \frac{4\pi a_0 W EM_c \beta_c F_0}{h N_e(r)} \times \int_{x_{El}}^{\infty} \frac{\exp[-(h\nu_{El}/kT_c)x - \theta_x(r)]}{x^{s+1}} dx. \quad (17)$$

This is our basic equation for the simplified theory describing the hot-corona-cool-wind model. The analysis nicely separates into two parts. The dependence on the electron temperature of the wind is confined to the left-hand side. The abundance of the parent ion $g(El^P)$ will depend on the local electron temperature through the diffuse radiation field. On the right-hand side are the simple functions of radius, W , N_e , and $\theta_x(r)$, along with the coronal parameters T_c and EM_c . The abundance of the "anomalous" ionization state $g(El^{P+2})$ is directly proportional to the coronal emission measure, and has a rather simple dependence on the coronal temperature. As discussed earlier, the coronal flux has a knee at $h\nu/kT_c = 1$. If $h\nu_{El}/kT_c \gg 1$, there will be negligible radiation beyond the K-shell edge and little of the El^{P+2} stage of ionization will be produced. As T_c increases, the production rate in-

creases rapidly. It should be possible, in fact, to deduce limits on coronal temperature by noting which elements have enhanced ionization and which do not.

The emission measure of the corona, EM_c , is not known *a priori*, but it is possible to put reasonable limits on it, if we expect it to be "thin" in comparison with the scale of the flow. As we are willing to specify the velocity and density structure in the cool wind, it is possible to derive an emission measure for the wind region, EM_w ,

$$EM_w = \int_{R_c}^{\infty} N_e^2 4\pi r^2 dr, \quad (18)$$

where R_c is the radius at the top of the coronal region where $v(R_c) = v_0$. Applying the transformation of equation (12) to equation (18), we convert the spatial integral to a velocity integral. Assuming hydrogen and helium to be completely ionized so that $N_e \propto \dot{M}/v r^2$, this integral gives

$$\begin{aligned} EM_w &= \left(\frac{\dot{M}}{4\pi\mu_e m_H} \right)^2 \frac{8\pi}{v_1^2 R_c} \ln(v_\infty/v_0) \\ &= 2.32 \times 10^{59} \left(\frac{\dot{M}}{10^{-6}} \right)^2 \left(\frac{R_\odot}{R_c} \right) \left(\frac{1000}{v_1} \right)^2 \ln \left(\frac{v_\infty}{v_0} \right), \end{aligned} \quad (19)$$

where \dot{M} is in solar masses per year, v_1 is in km s^{-1} , and μ_e is the mean particle mass per electron. The emission measure of the coronal region is expected to scale with \dot{M} and R_c in the same way as does EM_w . Therefore we let

$$EM_c = \gamma_c EM_w,$$

where γ_c is our new adjustable parameter and we expect that a thin corona will have $\gamma_c < 1$. For ζ Pup one has $EM_w \approx 2.5 \times 10^{59} \text{ cm}^{-3}$.

Table 3 shows the results of solutions of equation (17) for the radial distribution of Auger ionization for the case in which $T_c = 5 \times 10^6$ and $\gamma_c = 0.1$. Results are given for five elements which have resonance lines in the ultraviolet that might be enhanced by the Auger process: C, N, O, Si, and S. If we assume that oxygen is mostly in the ionization stage O^{+3} , then the amount of O^{+5} at $2 R_*$ produced by the Auger mechanism is near that required to fit

TABLE 3

RESULTS OF SIMPLIFIED THEORY FOR THE RATIO $g(El^{P+2})/g(El^P)$ IN AN OPTICALLY THICK WIND OF ζ PUPPIS*

r/R_*	C	N	O	Si	S
1.1 . . .	-2.43	-2.53	-2.54	-2.51	-3.33
1.2 . . .	-2.66	-2.76	-2.77	-2.49	-3.27
1.5 . . .	-2.93	-3.03	-3.05	-2.49	-3.22
2.0 . . .	-3.10	-3.20	-3.22	-2.50	-3.20
5.0 . . .	-3.29	-3.40	-3.41	-2.53	-3.18
10.0 . . .	-3.34	-3.44	-3.46	-2.54	-3.18

* Parameters: $T_{\text{eff}} = 42,000 \text{ K}$, $T_c = 5 \times 10^6 \text{ K}$, $\dot{M} = 8 \times 10 M_\odot \text{ yr}^{-1}$, $\log EM_w = 59.4$, $\log EM_c = 58.4$.

the observations shown in Table 2. Thus we conclude from the simplified theory that for ζ Pup, $EM_c = 2.5 \times 10^{58}$. This agrees well with the detailed analysis presented in the following section and with the analysis of Olson (1978). This value of EM_c required for the optically thick case is about two orders of magnitude larger than that required if the wind were optically thin.

Note also in Table 3 that $g(EI^{P+2})$ decreases in the outward radial direction, in contrast with the optically thin case. This effect is entirely due to the attenuation factor $\exp[-\theta_v(r)]$. In the thin case the higher stages of ionization should increase outwardly, in proportion to $v(r)$, as discussed earlier.

The abundance of O^{+5} can also be increased by increasing the coronal temperature. This is shown in Figure 2, which is a plot of $g(EI^{P+2})/g(EI^P)$ versus coronal temperature for C, N, and O. For oxygen, one gets an increase in the abundance of O^{+5} by an order of magnitude, if the coronal temperature is increased from 5×10^6 to about 12×10^6 K. Although one could increase either the coronal temperature or coronal emission measure to enhance the high stage of ionization, we will continue to consider in detail only the case in which the coronal temperature is 5×10^6 K.

Some aspects of this simplified theory will be referred to in § IV, but we must discuss in somewhat more detail the processes that influence the dominant stage of ionization.

b) The Effect of the Diffuse Field on the Ionization Conditions in ζ Puppis

The results of the previous section have shown that O^{+5} can be produced in a spatially extended region in ζ Pup, in spite of the fact that the wind is very thick at the O^{+4} to O^{+5} ionization edge and at the K-shell edge of O^{+3} . This is because the wind becomes optically thin at frequencies well beyond the K-shell edge. Coronal X-rays at those frequencies can produce sufficient Auger ionization for the production of O^{+5} in ζ Pup and other ions in cooler stars. Thus we have overcome the objection of Natta *et al.* (1975) to models having coronal radiation produced only near the base of the wind. In this section we will treat the problem in somewhat greater detail and investigate the dependence of the ionization structure of the wind on the electron temperature in the wind. The opacity of the wind material depends on the electron temperature through the collisional ionization and recombination rates, and the dilute radiation field depends on the electron temperature through $B_v(T_e)$. The actual run of electron temperature is determined by the radiative equilibrium condition, in the hybrid corona plus cool wind picture, but as discussed in Klein and Castor (1978) the determination of the radiative equilibrium temperature is a very difficult problem. Therefore we consider several isothermal models with appropriately "cool" temperatures.

In particular we consider three cases: $T_e = 30,000$, 35,000, and 40,000 K, which are in the range of tem-

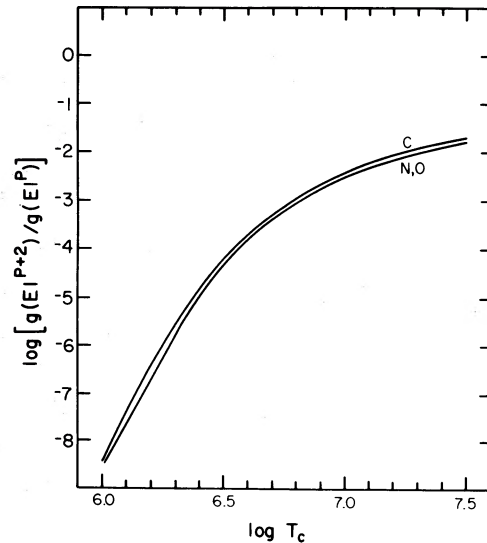


FIG. 2.—Shows the ratio of the relative abundance of two stages of ionization EI^{P+2} and EI^P that is caused by the Auger process for several elements, as a function of assumed coronal temperature T_e . In the calculations leading to these results, the optical depth of the wind of ζ Pup is accounted for, and it is assumed that $EM_c = 10^{58.4} \text{ cm}^{-3}$ and that the coronal emission varies with temperature as $\exp(-h\nu/kT_e)$.

peratures appropriate for a gas in radiative equilibrium. In our calculation of the radiation field we take into account the outer-shell and K-shell ionization opacities of He, C, N, O, Ne, Mg, Si, and S.

The ionization equilibrium matrix equation for each chemical element is solved as described in § II, but now we must include in the photoionization rates a contribution from a mean intensity $J_v(r)$ that accounts for the attenuated stellar plus coronal flux and for the locally produced diffuse radiation field.

At frequencies for which the wind is optically thin, J_v is the spatially diluted stellar plus coronal flux, WF_v . At frequencies for which the wind is very thick, the intensity is the local source function which we take to be $B_v(T_e)$, the Planck function at the local electron temperature. As an interpolation between these two extremes we actually use in the radiative ionization rate equations

$$J_v(r) = WF_v \exp(-\theta_v) + B_v(T_e) \times [1 - 0.5 \exp(-\theta_v) - 0.5 \exp(-\tau_v)], \quad (20)$$

where θ_v is the optical depth from the top of the coronal zone, R_c to r :

$$\theta_v = \int_{R_c}^r \kappa_v \rho dr;$$

and τ_v is the optical depth from r to infinity:

$$\tau_v = \int_r^{\infty} \kappa_v \rho dr.$$

The expression for the diffuse contribution to J_v in equation (20) is just a two-stream or "flare approxima-

tion" used in solar work and is meant to describe in a simple way the contribution to the diffuse radiation from the wind interior to r and from the wind exterior to r , i.e.,

$$J_\nu^d(r) \approx \frac{1}{2}B_\nu[1 - \exp(-\theta_\nu)] + \frac{1}{2}B_\nu[1 - \exp(-\tau_\nu)].$$

This is rather crude, and one could consider slightly more sophisticated angle averages as in Olson (1978). However, it certainly leads to an adequate representation of the spatial dependence of the ionization just above a coronal region. We feel that it is appropriate in light of the other simplifying approximations of the model, such as our simple two-component temperature structure and the Planckian continuum distribution. At the frequencies which are required to produce O^{+5} from O^{+3} ($\geq 10^{17}$ Hz), the diffuse field contributes negligibly to the radiative rates as can be seen in Figure 1, which shows the rapid decline of $B_\nu(T_e)$ for $T_e = 35,000$ K. For the source function of the optically thick wind, we are using $S_\nu = B_\nu(T_e)$. This is quite adequate for the case in which the electron temperature and the temperature of the incoming radiation field are nearly equal. More generally one might use $S_\nu = B_\nu/b_1$, where b_1 is the departure coefficient for the ground level of He^+ or whatever ion is the dominant source of opacity, as discussed by Klein and Castor (1978). These authors have discussed the formidable problems associated with the determination of b_1 and have concluded that b_1 is within an order of magnitude of unity if the electron temperature and radiation temperature are nearly the same. A change in b_1 by a factor of 10 corresponds, for example, to a change in the diffuse radiation temperature of only about 11% at 35,000 K at the N^{+3} to N^{+4} edge at 192 Å. This change is well within the uncertainties of the temperature of the radiative equilibrium wind.

The spatial distribution of the ionization is calculated in the process of finding the attenuation optical depth θ_ν . We numerically integrate the differential equation

$$\frac{d\theta_\nu}{dr} = \kappa_\nu \rho = \sum_{El} \sum_j N_{El,j} a_\nu(El, j), \quad (21)$$

starting at the top of the coronal zone (i.e., the base of the cool wind) where $\theta_\nu = 0$. The monochromatic opacity κ_ν is, as usual, the sum over the opacities of all the stages of ionization of all of the elements considered, including K-shell opacity. To get the number of particles in the j th stage of ionization for element El , it is necessary to know the radiation field $J_\nu(r)$ which in turn depends on $\theta_\nu(r)$. Therefore, the monochromatic optical depth calculations in equation (21) are coupled and the differential equations must be solved simultaneously. We have solved the simultaneous set of first-order differential equations using a variable step Hamming predictor corrector method which uses a Runge Kutta procedure to start the calculation. The expression for J_ν also involves the optical depth τ_ν . We found that it is adequate to

estimate τ_ν on the basis of the local value of κ_ν that is found at each step of the outward integration; thus we used

$$\tau_\nu(r) = \kappa_\nu(r) \frac{\dot{M}}{4\pi v_1^2 R_c} (v_\infty - v). \quad (22)$$

One could consider iterating to derive τ_ν , but the predicted value is found to agree with the value calculated on the outward integration to within about 30% at most frequencies and is therefore sufficiently accurate.

The results for the derived spatial distribution of the ionization in ζ Pup are shown in Figure 3 for three different wind temperatures with $EM_c = 10^{58} \text{ cm}^{-3}$. We find that the fractional abundance of O^{+5} decreases in the outward direction from values near 0.03 at the base of the cool wind to values near 10^{-4} very far from the star. So as to isolate the effects of the coronal radiation, the results for N^{+4} and O^{+5} are also shown in Figure 3 for the case with no corona, i.e., $EM_c = 0$. Note that the spatial distribution of C^{+2} and N^{+4} , beyond a thin region just above the corona, are controlled by the noncoronal radiation field, i.e., the ambient diffuse field and the strongly attenuated photospheric field. The required amounts of C^{+2} and N^{+4} (Table 2) are achieved for wind temperatures between 30,000 and 35,000 K. The wind is very thick (i.e., $\bar{\tau}_\nu = \tau_\nu + \theta_\nu > 10$) out to about 3×10^{17} Hz (Fig. 4), so $J_\nu \approx B_\nu$ throughout most of the wind. This explains the increase in the outward direction of the abundance of N^{+4} . For if $J_\nu \approx B_\nu$, the right-hand side of equation (7) is constant and thus the ratio of N^{+4} to the dominant stage N^{+3} increases as $1/N_e$. This also explains the rise in the abundance of O^{+5} for the case with $T_e = 40,000$ K (Fig. 3c) because at such temperatures O^{+4} is the dominant stage of ionization.

In Figure 3c, we see that the diffuse field produces significant amounts of O^{+5} beyond about $2 R_*$. This result partly illustrates the "tepid wind" explanation of the anomalous ionization in O stars that has been proposed by Castor (1978). If the winds of the OB stars from O4 through B0.5 are at temperatures higher than 40,000 K, the spectra should show the strong O^{+5} lines. This is certainly a feasible alternative to the warm-wind and hybrid coronal-plus-cool-wind models, and the other observable consequences of the tepid wind model are being investigated by Castor (1978). These three models are compared in a review by Cassinelli, Castor, and Lamers (1978).

In Figures 3a and 3b we see that the noncoronal field contributes a negligible amount of O^{+5} . (For the 30,000 K case, the contribution is below the graph and hence the $EM_c = 0$ case cannot be shown on Fig. 3a). We conclude from Figures 3a and 3b that the degree of ionization seen in O stars can be produced in a cool stellar wind, subjected to coronal X-ray radiation. So as to avoid any overlap of the coronal explanation and the tepid-wind explanation of the ionization, we will not consider the $T_e = 40,000$ K case any further but will focus our attention on the cooler winds and

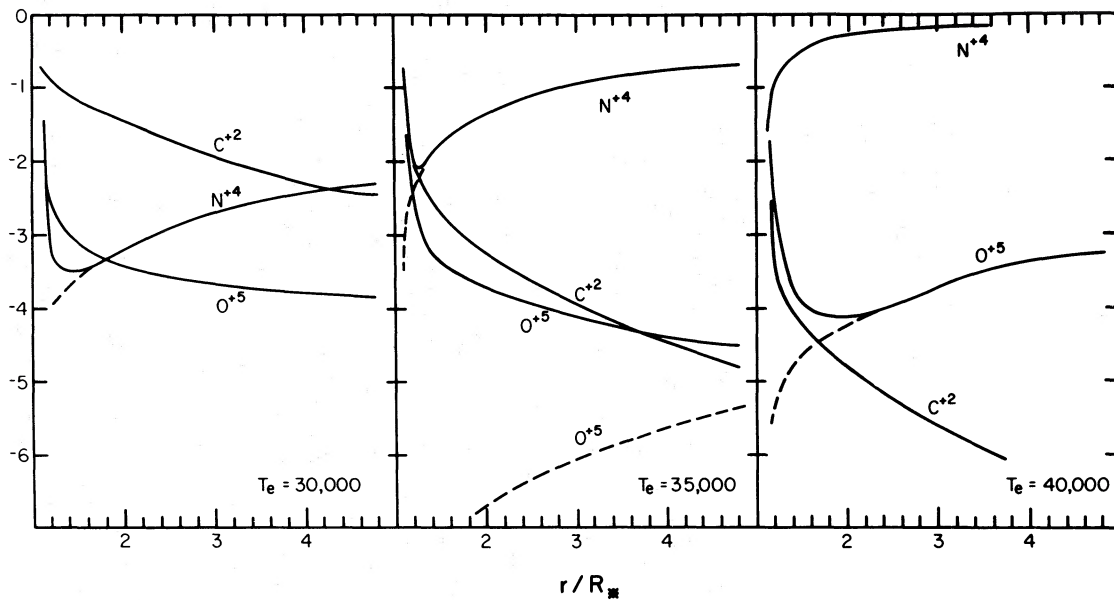


FIG. 3.—The relative degree of ionization of C^{+2} , N^{+4} , and O^{+5} versus radius in the optically thick wind of ζ Pup. Results are shown for isothermal winds with the three electron temperatures indicated in each section, and in each case the corona is assumed to have a temperature of 5×10^6 K and an emission measure of 10^{58} cm^{-3} . So as to isolate the effect of the coronal radiation from that of the dilute radiation field, shown in dashed lines are results for N^{+4} and O^{+5} for the case in which there is no coronal emission, i.e., $EM_c = 0.0$. At 30,000 K one should expect negligible O^{+5} unless coronal radiation is present; at 40,000 K the diffuse field alone can produce significant O^{+5} .

discuss the expected X-ray emission and compare it with available observations.

For the ζ Pup model we have found that a coronal model with an emission measure of about 10^{58} cm^{-3} can produce the needed degree of ionization in a wind with a gas temperature of about $30\text{--}35 \times 10^3$ K. The X-ray luminosity that is transmitted through the entire flow region is $L_v^* \exp(-\tau_v)$, where L_v^* is the sum of the photospheric and coronal luminosities. The total

optical depth, τ_v , of the wind of ζ Pup is shown in Figure 4 as a function of frequency. At very large energies, the K shell opacity of carbon, nitrogen, and oxygen is seen to dominate, as was assumed in the simplified theory discussed before. The emergent radiation field is shown in Figure 5, for the two wind temperature $T_e = 30,000$ and $35,000$ K.

The X-ray flux falls slightly below the *ANS* channel 4 upper limits, and hence we cannot rule out coronal models on the basis of current observational data. At the channel 1 energies of ~ 0.25 keV there is now a greatly diminished flux owing to the metallic photoionization opacities in the wind. Although there are several uncertainties in our calculated model and in our estimates of the interstellar optical depths, one can safely conclude that instruments only slightly more sensitive than those on the *ANS* satellite will be able to prove the existence or absence of a corona around ζ Pup. The *HEAO B* satellite scheduled for launch in late 1978 will have the required sensitivity and spatial resolution to do this.

We suggest that attempts should also be made to detect a flux at $\frac{1}{4}$ keV for several reasons. The flux at these wavelengths is somewhat model dependent. For example, we have seen that the optically thin model showed a significant $\frac{1}{4}$ keV flux. The calculated optical depth depends somewhat on the assumed velocity structure, and the velocity at the base of the cool wind. If we assume that the velocity at the base of the wind is 500 km s^{-1} instead of the $v_\infty/20$ that we used through the rest of the modeling, the $\frac{1}{4}$ keV flux is increased by an order of magnitude, though still well below the *ANS* channel 1 limit. Hearn (1975) suggested that the winds of early type stars are driven

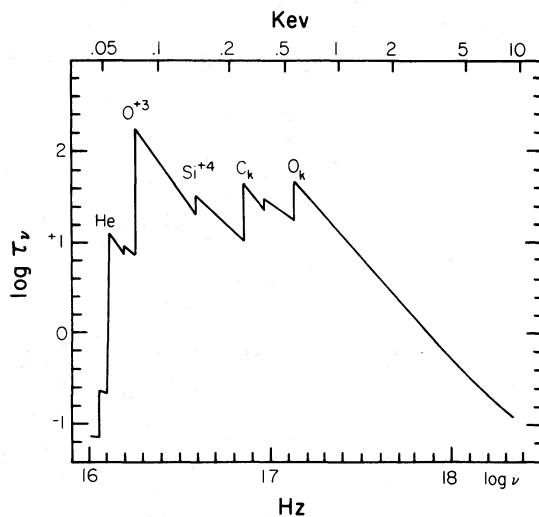


FIG. 4.—Shown is the total optical depth of the wind at frequencies beyond the He II edge. Also indicated are important opacity edges of oxygen and silicon and K-shell edges of C and O. At large frequencies the optical depth decreases as $\nu^{-2.6}$.

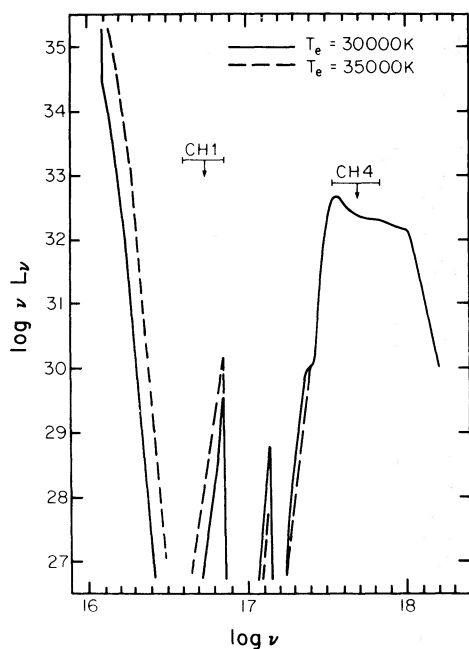


FIG. 5.—The emergent X-ray spectrum expected for ζ Pup, after accounting for the attenuation by the cool wind. These results correspond to the case with $T_e = 5 \times 10^6$ K, $EM_e = 10^{28}$, and two values for the wind electron temperature, T_e , as indicated. The X-ray upper limits from two of the *ANS* channels are also shown. At very large frequencies the emergent flux is nearly independent of the assumed electron temperature because the opacity is primarily K-shell absorption.

to nearly escape velocities by a coronal zone; thus the relative flux at $\frac{1}{4}$ keV and 2 keV could perhaps provide a test of that type of model. Such a model has already been criticized by Cassinelli, Olson, and Stalio (1978) on the basis of observed $H\alpha$ lines contours, but other evidence for or against the model would be useful.

IV. THE ANOMALOUS IONIZATION IN THE WINDS OF OB SUPERGIANTS

Anomalous ionization in stellar winds is not confined to ζ Pup and other Of stars but extends to B supergiants, as can be seen in the catalog of Snow and Morton (1976), and as discussed by Lamers and Snow (1978). The O^{+5} ion is observed in the winds of supergiants as late as κ Ori (B0.5 Ia, $T_{\text{eff}} \approx 26,400$ K). Recently Morton (1978) has studied the presence of O^{+5} in a range of stars and has found that it is absent in the B1 supergiants ρ Leo and γ Ara ($T_{\text{eff}} \approx 21,000$ K) and in later spectral types. The N^{+4} ion persists to somewhat later supergiants, as it is present in ρ Leo (B1 Iab) (Snow and Morton 1976), is weak in θ Ara (B2 Ib) (Savage 1978; Upson 1978) with $T_{\text{eff}} \approx 18,000$ K, and is absent at B3 I and later. The *Copernicus* satellite has a low sensitivity to wavelengths near the C^{+3} doublet at 1550 \AA , but several observations have been made from *Skylab* and were reported by Parsons *et al.* (1978). The C^{+3} ion exists in winds of stars at least as late as σ^2 CMa (B3 Ia) with $T_{\text{eff}} = 15,500$ K. The Si^{+3} ion is evidenced in stars as late as β Ori

(B8 Ia, $T_{\text{eff}} = 12,000$ K). In this section we will discuss the possibility that all of these anomalies can be explained by the corona-plus-cool-wind model. An alternate explanation in terms of the warm wind model was presented by Lamers and Snow (1978), who postulated that stars showing O VI have winds with $T_e = 2 \times 10^5$ K and later B supergiants have winds with $T_e = 8 \times 10^4$ K.

a) Ionization Stages Expected in OB Supergiant Winds and Predictions of the Auger Ionization Model

In the corona-plus-cool-wind model the anomalously high ionization stages are expected to be produced by K-shell ionization of the dominant ion. Therefore we must first determine the dominant stages that are expected to exist in the winds of the O and B supergiants. These stars have effective temperatures ranging from 42,000 K for the early O stars down to about 10,000 K for the late B supergiants. To get a rough estimate as to which stages of ionization are dominant in which stars, we have solved the ionization equilibrium equations for gases with $T_e = 0.8 T_{\text{eff}}$, and with an electron density $N_e = 10^{10} \text{ cm}^{-3}$, which is rather typical of stellar wind densities. We have carried out the calculations in two ways: first, we assumed that the winds are very thick and therefore the mean intensity is given by $J_\nu = B_\nu(T_e)$. Second, we assumed that the radiation field is that of a dilute photospheric field at $r = 2 R_*$, i.e., $J_\nu = WF_\nu^*$, where F_ν^* is the photospheric flux. For F_ν^* we used the results of the model calculations of Kurucz, Peytremann, and Avrett (1974), for effective temperature in the range 10,000–45,000 K, and $\log g = 4.5$. The results for carbon and oxygen are shown in Figure 6, and similar results were obtained for the other elements of interest. From such graphs we read off two temperature ranges: the temperature range in which a given ion has a relative abundance of at least 10^{-4} , and is therefore likely to be observable in its strong resonance lines; and the temperature range in which the ion is one of the “dominant” stages, i.e., having a relative abundance greater than 10%. These latter ions are the ones that we can expect to be likely “parents” for an anomalously high stage of ionization because of K-shell absorption and subsequent Auger ionization. The effective temperature ranges for which we expect a given ion to have relative abundances of $g > 10^{-4}$ or $g > 10^{-1}$ are summarized in Table 4.

Table 5 lists seven sets of ultraviolet lines from high stages of ionization that are included in the list of Snow and Morton (1976) of “lines most likely to reveal mass loss.” Their data for the lines and atomic abundances are repeated in this table. Column (5) gives the range in effective temperature for which the ion has an abundance of 10^{-4} and is likely to be seen. This range is taken from the data of Table 4. Note, for example, that the O VI doublet is not expected to be seen in the spectra of any of the O and B stars, and N V and S VI should be seen only in the hottest Of stars. In column (6) is listed the effective temperature range in which we expect the line to be anomalously strong

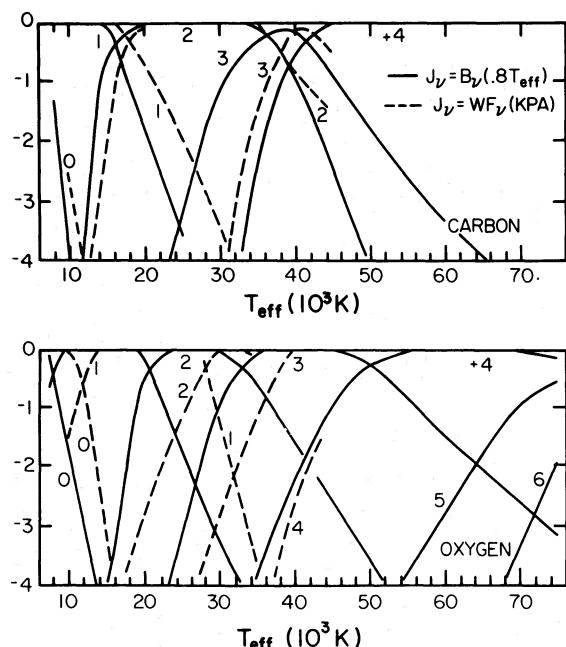


FIG. 6.—Shows the ionization equilibrium of carbon and oxygen versus effective temperature of the supergiant with a stellar wind, at a place where the wind electron density is $1 \times 10^{10} \text{ cm}^{-3}$. The calculations were carried out for two “limiting” approximations for the mean intensity J_ν . First, J_ν was assumed to be the diffuse radiation field of a very optically thick wind which has an electron temperature of $0.8 T_{\text{eff}}$. These results are indicated by the solid lines. Second, the mean intensity was assumed to be that in an optically thin wind, and thus is the diluted radiation field of the stellar photosphere. These results are shown by the dashed lines. The photospheric flux F_ν was taken from the tables of Kurucz, Peytremann, and Avrett (1974), and the dilution factor is for a radius of $2 R_*$.

owing to the Auger process. In deriving this we have simply assumed that the K-shell ionization will lead to the ejection of two electrons from a parent ion. Thus the relevant temperature range is the one in which the parent is one of the “dominant” stages, as given in Table 4. Column (7) of Table 5 identifies the parent ion, and the K-shell ionization edge for that ion is given in column (8), and is taken from Daltabuit and Cox (1972).

Note that we expect the Auger process to lead to strong lines of C IV and Si IV in the winds of supergiants with effective temperatures as low as about 10,000 K, whereas normally these lines should not be expected in stars with effective temperatures less than 20,000 K. The lines of N V and O VI are expected to be anomalously strong in stars with T_{eff} greater than 20,000 K and 30,000 K, respectively.

b) Comparison of Predictions and Observations

Table 6 summarizes the results of the observational surveys discussed above. Listed are nine O and B supergiants with effective temperatures ranging from that of ζ Pup, 42,000 K, down to the 11,600 K of β Ori. Asterisks indicate that the indicated resonance line is actually seen with a P Cygni or shortwardly displaced absorption feature and is therefore formed in the stellar wind. Daggers indicate lines that are not expected in the cool radiative equilibrium wind around the star. Finally, the range in effective temperatures over which one might expect to see the line significantly enhanced by the Auger process is indicated by a double dagger (\ddagger). These predictions are based on the results in Table 5.

If the Auger ionization model is correct for all of the OB supergiants, one should expect to see nothing

TABLE 4
SUMMARY OF IONIZATION EQUILIBRIA CALCULATIONS: $N_e = 10^{10}$, $T_e = 0.8 T_{\text{eff}}$, AND $J_\nu = B_\nu(T_e)$ OR [$J_\nu = W F_\nu(T_{\text{eff}})$]

Ion	I^* ΔT_{eff}	II^\ddagger ΔT_{eff}	Ion	I^* ΔT_{eff}	II^\ddagger ΔT_{eff}	Ion	I^* ΔT_{eff}	II^\ddagger ΔT_{eff}
C ⁺¹	8– 18 (< 10– 21)	< 8– 27 (< 10– 32)	O ⁺²	20– 37 (26– 39)	16– 52 (18–> 45)	P ⁺²	13– 25 (15– 32)	10– 40 (10– 37)
C ⁺²	15– 40 (16– 40)	12– 50 (13–> 45)	O ⁺³	30– 56 (36–> 45)	24– 75 (28–> 45)	P ⁺³	20– 42 (26– 44)	15– 52 (18–> 45)
C ⁺³	30– 46 (37–> 45)	23– 65 (31–> 45)	O ⁺⁴	45–> 75 (... ..)	35– 75 (38– 45)	P ⁺⁴	34– 48 (37–> 45)	25– 71 (32–> 45)
C ⁺⁴	39–> 75 (40–> 45)	34–> 75 (36–> 45)	O ⁺⁵	70–> 75 (... ..)	54– ... (... ..)	P ⁺⁵	40–> 75 (40–> 45)	34–> 75 (37–> 45)
N ⁺¹	8– 20 (11– 27)	< 8– 30 (< 10– 33)	Si ⁺¹	< 8– 13 (< 10– 16)	< 8– 22 (< 10– 26)	S ⁺¹	< 8– 17 (< 10– 20)	< 8– 25 (< 10– 30)
N ⁺²	17– 35 (26– 39)	14– 50 (18–> 45)	Si ⁺²	11– 28 (14– 32)	8– 35 (11– 37)	S ⁺²	14– 29 (16– 33)	11– 29 (12– 41)
N ⁺³	28– 60 (37–> 45)	22– 74 (29–> 45)	Si ⁺³	22– 34 (30– 37)	19– 48 (22– 45)	S ⁺³	23– 43 (28– 45)	16– 57 (22–> 45)
N ⁺⁴	50– 67 (> 45– ...)	38–> 75 (40–> 45)	Si ⁺⁴	28–> 75 (33–> 45)	23– 75 (30– 45)	S ⁺⁴	30– 59 (36–> 45)	24– 70 (32–> 45)
O ⁺¹	8– 23 (12– 29)	< 8– 32 (10– 35)	P ⁺¹	8– 16 (< 10– 18)	< 8– 23 (< 10– 28)	S ⁺⁵	46– 64 (> 45– ...)	36–> 75 (39–> 45)

* Column I: Effective temperature range (ΔT_{eff}) in 10^3 K for which $N_{\text{ion}}/N_{\text{element}} > 0.1$.

† Column II: Effective temperature range (ΔT_{eff}) in 10^3 K for which $N_{\text{ion}}/N_{\text{element}} > 1.0 \times 10^{-4}$.

TABLE 5
ULTRAVIOLET RESONANCE LINES LIKELY TO BE ENHANCED BY AUGER IONIZATION

Line (1)	λ (\AA) (2)	f (3)	Abundance $N_{\text{EI}}/N_{\text{H}}$ (4)	T_{eff} Range Normally Expected (10^3 K) (5)	T_{eff} Range Ion Expected via Auger Process (10^3 K) (6)	Parent Ion (7)	K-Shell Edge (keV) (8)
C IV.....	1548.2 1550.8	0.194 0.097	3.7×10^{-4}	26-65	9-20	C ⁺	0.296
N V.....	1238.8 1242.8	0.152 0.076	1.1×10^{-4}	$T_{\text{eff}} > 39$	20-37	N ⁺	0.432
O VI.....	1031.9 1037.6	0.130 0.065	6.8×10^{-4}	$T_{\text{eff}} > 54$	30-50	O ⁺	0.595
Si IV.....	1393.8 1402.8	0.528 0.262	3.5×10^{-5}	20-45	8-16	Si ⁺	1.88
P V.....	1118.0 1280.0	0.495 0.245	2.7×10^{-7}	33-70	14-29	P ⁺	2.24
S IV.....	1062.7 1073.0	0.038 0.037	1.6×10^{-5}	19-50	8-19	S ⁺	2.54
S VI.....	933.4 944.5	0.426 0.210	1.6×10^{-5}	$T_{\text{eff}} > 37$	25-44	S ⁺	2.58

but asterisks or dagger symbols at and above the double dagger and only § symbols below the double dagger.

The predictions of the theory hold up amazingly well for Si IV, C IV, N V, and O VI. There is only one striking departure from the predictions of the model. The sulfur lines, S IV and S VI, show no anomalous enhancements, i.e., no dagger in the table. This is easily explained because the S IV lines should be 30 times weaker than the Si IV lines when relative abundances and oscillator strengths are considered, thus S IV λ 1065 is too weak to show the Auger enhancement except possibly in B supergiants with very strong winds. For similar reasons the S VI lines should be 10 times weaker than the O VI lines. Furthermore, the lines are in the short wavelength region that has either not been observed or not yet published. The catalog of Snow and Jenkins (1977) starts at 1000 \AA . Phosphorous shows little enhancement, but this can be explained by its low abundance.

c) *The Absence of O VI in the Spectra of Supergiants of Type B1 and Later*

In the corona-plus-cool-wind model the O⁺ ion is produced from O⁺ by the Auger mechanism. At temperatures somewhat below 30,000 K, the O⁺ stage ceases to be the dominant stage of ionization. Thus one should expect a rather sharp decrease in the strength of O VI as one looks at supergiants of spectral type later than B0.

We have carried out several of the detailed calculations described in the previous section for a star with an effective temperature of 25,000 K. The results are shown in Figure 7, in which the abundance of N⁺ and O⁺ is plotted versus radius, for two values of the electron temperature, $T_e = 20,000$ and 25,000 K, for two values for the volume emission measure, $\log EM_c = 56.4$ and 57.4, and for $T_c = 5 \times 10^6$ K. The volume emission measure for the cool wind, using parameters appropriate for ρ Leo, calculated as before

TABLE 6
RESONANCE LINES SEEN FROM HIGH STAGES OF IONIZATION IN OB SUPERGIANTS

Star	T_{eff} (K)	\dot{M} ($10^{-6} M_{\odot} \text{ yr}^{-1}$)	S IV λ 1065	Si IV λ 1400	C IV λ 1550	P V λ 1120	N V λ 1240	O VI λ 1035	S VI λ 940
ζ Pup, O4f.....	42,000	7.0	*	*	*	*	*	†	*
α Cam, ζ Ori, O9.5 Ia....	30,000	2.5	*	*	*	*	†	†	...
ϵ Ori, B0 Ia.....	24,800	4.3	*	*	*	...	†	†	...
	28,800								
κ Ori, B0.5 I.....	26,400	2.5	*	*	†	††	...†
ρ Leo, B1 Iab.....	21,000	1.0	(*)	*	††	§	...
θ Ara, B2 Ib.....	18,000	††	§§	...
σ^2 CMa, B3 Ia.....	15,500	2.0	§	†	†	...†	§	§§	...
η CMa, B5 Ia.....	13,300	0.4	§	†	(§)	...	§	§§	...
γ Ori, B8 Ia.....	11,600	1.0	†§	††	...†

* The line shows mass loss effects; P Cygni profile or displaced absorption.

† This line is not expected in a cool radiative equilibrium wind, yet is seen.

†† Coolest star for which Auger enhancement is expected for the line.

§ The line shows no mass loss effects.

NOTE.—Three dots (...) indicate no information; () indicates an uncertainty.

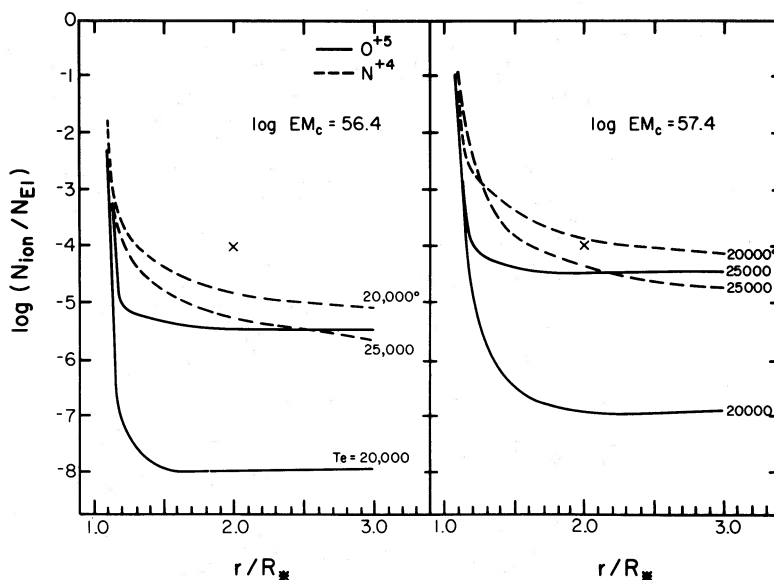


FIG. 7.—Shown are the relative abundances of N^{+4} and O^{+5} versus radius in the wind of a supergiant with an effective temperature of 25,000 K for two values for the coronal emission measure. The far-ultraviolet flux from the photosphere was assumed to be that of a blackbody at 25,000 K, and the coronal flux was assumed to be that of a gas at $T_c = 5 \times 10^6$ K as shown in Fig. 1. The attenuation and diffuse radiation field of the optically thick wind were accounted for. Results are shown for wind electron temperatures of 2×10^4 and 2.5×10^4 K. The \times is an indication of the abundance of these ions at $2 R_*$ that is required to produce significant absorption in the wind.

for ζ Pup using $v_0 = (1/20)v_1$, is $\log EM_w = 10^{58}$. Thus for either of the two parts of Figure 7, the thin corona restriction that $EM_c \ll EM_w$ is satisfied. In Figure 7b, abundances as large as 10^{-4} are achieved if the electron temperature in the wind is 25,000 K. One could expect an observable amount of O VI with a somewhat lower electron temperature by further increasing the coronal emission measure, or by increasing the coronal temperature.

We therefore conclude that the O^{+5} could be present in winds only with effective temperatures greater than 25,000 K.

The reason we first carried out this more detailed analysis was to try to understand the report by Lamers and Snow (1978) that both O VI and N V are in the spectrum of ρ Leo (B1 Iab), with $T_{\text{eff}} = 21,000$ K. Due to its low effective temperature there should be negligible O^{+3} in the wind of this star, and hence O^{+5} could not be produced by the Auger mechanism. More recently, Morton (1978) critically analyzed high-resolution *Copernicus* scans of ρ Leo and concluded that O VI was not present. Thus the corona-plus-cool-wind model successfully explains all the ionization anomalies in Of and OB supergiants from O4 to B8, as listed in Table 6.

V. SUMMARY

We have derived the ionization conditions expected in a cool wind of ζ Pup that is subjected to hard radiation from a coronal zone. We have found that the required degree of ionization of O VI can be produced even when the opacity of the stellar wind is accounted for. Therefore it is not necessary for the

hot gas to be distributed in extended filaments as suggested by Natta *et al.* (1975). The emergent X-ray flux has also been calculated and found to lie near but below the upper limits of the *ANS* satellite. Observations from the *HEAO B* satellite should be able to detect the X-rays expected to be emergent from ζ Pup, and thus prove or disprove the correctness of the corona-plus-cool-wind model.

To see if the corona-plus-cool-wind model could explain other ionization anomalies, we developed a simplified analysis of the Auger ionization process and applied it to B supergiants. The Auger ionizations tend to produce anomalously large abundances of ions that are two stages higher than the dominant stage(s). We estimated the expected dominant stages as a function of the effective temperature of B supergiants and predicted temperature ranges over which various resonance lines should be "anomalously" strong. The results explain very well the persistence to low effective temperatures of the strong lines of O VI, N V, C IV, and Si IV.

We are grateful to Dr. Rolf Mewe for permitting us to use his unpublished summary of *ANS* results and to Dr. Donald Cox for discussions concerning radiative ionization processes. We thank Walter Upson and Blair Savage for use of unpublished spectra of θ Ara. We have benefited greatly from many lively discussions of this work with Drs. David Abbott, John Castor, Henny Lamers, and Nino Panagia. We also wish to thank Anne Underhill and Lowell Doherty for comments on earlier versions of the manuscript. This work was supported in part by National Science Foundation grant AST 76-15448.

REFERENCES

- Aldrovandi, S. M. V., and Péquignot, D. 1973, *Astr. Ap.*, **25**, 137.
- Bohlin, R. C. 1975, *Ap. J.*, **200**, 402.
- Bohlin, R. C., Harrington, J. P., and Stecher, T. P. 1978, preprint.
- Cassinelli, J. P., and Hartmann, L. 1977, *Ap. J.*, **212**, 488.
- Cassinelli, J. P., Olson, G. L., and Stalio, R. 1978, *Ap. J.*, **220**, 573.
- Cassinelli, J. P., Castor, J. I., and Lamers, H. J. G. L. M. 1978, *Publ. Astr. Soc. Pac.* **90**, 477.
- Conti, P. S., and Frost, S. A. 1977, *Ap. J.*, **212**, 728.
- Castor, J. I. 1978, in *IAU Symposium No. 83, Mass Loss and Evolution of O-Type Stars*, ed. P. S. Conti and C. de Loore (Dordrecht: Reidel), in press.
- Cruddace, R., Paresce, F., Bowyer, S., and Lampton, M. 1974, *Ap. J.*, **187**, 497.
- Daltabuit, E., and Cox, D. E. 1972, *Ap. J.*, **177**, 855.
- Davis, J., Morton, D. C., Allen, L. R., and Hanbury Brown, R. 1970, *M.N.R.A.S.*, **150**, 45.
- Giacconi, R., Murray, S., Gursky, H., Kellogg, E., Schreier, E., Matilsky, T., Koch, D., and Tanabaum, H. 1974, *Ap. J. Suppl.*, **237**, 27.
- Hearn, A. G. 1975, *Astr. Ap.*, **40**, 277.
- Holm, A. C., and Cassinelli, J. P. 1977, *Ap. J.*, **211**, 432.
- Hummer, D. C. 1977, paper presented at IAU Symp. 76 on Planetary Nebulae, to be published.
- John, T. L., and Morgan, D. J. 1974, *J. Quant. Spectrosc. Rad. Transf.*, **14**, 777.
- Kato, T. 1976, *Ap. J. Suppl.*, **30**, 397.
- Kirkpatrick, R. C. 1972, *Ap. J.*, **176**, 381.
- Klein, R. I., and Castor, J. I. 1978, *Ap. J.*, **220**, 902.
- Kurucz, R. L., Peytremann, E., and Avrett, E. H. 1972, *Blanketed Model Atmospheres for Early Type Stars* (Washington: Smithsonian Institution Press).
- Lamers, H. J. G. L. M. 1975a, private communication.
- Lamers, H. J. G. L. M., and Morton, D. C. 1976, *Ap. J. Suppl.*, **32**, 715.
- Lamers, H. J. G. L. M., and Rogerson, J. B. 1978, *Astr. Ap.*, in press.
- Lamers, H. J. G. L. M., and Snow, T. P. 1978, *Ap. J.*, **219**, 504.
- Mewe, R. 1976, private communication.
- Mewe, R., Heise, J., Gronenschild, E. H. B. M., Brinkman, A. C., Schrijver, J., and den Boggende, A. J. F. 1975, *Ap. J. (Letters)*, **202**, L67.
- Morton, D. C. 1978, in *IAU Symposium No. 83, Mass Loss and Evolution of O-Type Stars*, ed. P. S. Conti and C. de Loore (Dordrecht: Reidel), in press.
- Morton, D. C., and Dinerstein, H. L. 1976, *Ap. J.*, **204**, 1.
- Morton, D. C., and Wright, A. E. 1978, *M.N.R.A.S.*, **182**, 47P.
- Natta, A., Priete-Martinez, A., Panagia, N., and Macchetto, F. 1975, Laboratorio di Astrofisica Spaziale, Internal Rept. No. 23.
- Olson, G. L. 1978, *Ap. J.*, **226**, 124.
- Osterbrock, D. E. 1974, *Astrophysics of Gaseous Nebulae* (San Francisco: Freeman).
- Parsons, S. B., Wrays, J. D., Henize, K. G., and Benedict, D. F. 1978, preprint.
- Reynolds, R. J. 1976, *Ap. J.*, **203**, 151.
- Savage, B. D. 1978, private communication.
- Seaton, M. J. 1964, *Planet. Space Sci.*, **12**, 55.
- Snow, T. P., and Jenkins, E. B. 1977, *Ap. J. Suppl.*, **33**, 269.
- Snow, T. P., and Morton, D. C. 1976, *Ap. J. Suppl.*, **32**, 429.
- Upson, W. L. 1978, private communication.
- Weisheit, J. C. 1974, *Ap. J.*, **190**, 735.
- Withbroe, G. L. 1971, *The Menzel Symposium*, ed. K. B. Gebbie (NBS Spec. Pub. 353), p. 127.

JOSEPH P. CASSINELLI: Washburn Observatory, University of Wisconsin-Madison, Madison, WI 53706

GORDON L. OLSON: Free University of Brussels, 1050 Brussels, Belgium